

Optimal Control of a Fishery Utilizing Compensation and Critical Depensation Models

Mahmud Ibrahim

Department of Mathematics, University of Cape Coast, Cape Coast, Ghana

Received: 12 Dec. 2019, Revised: 2 Jan. 2020, Accepted: 15 Feb. 2020

Published online: 1 May 2020

Abstract: This study proposes optimal control problems with two different biological dynamics: a compensation model and a critical depensation model. The static equilibrium reference points of the models are defined and discussed. Also, bifurcation analyses on the models show the existence of transcritical and saddle-node bifurcations for the compensation and critical depensation models respectively. Pontryagin's maximum principle is employed to determine the necessary conditions of the model. In addition, sufficiency conditions that guarantee the existence and uniqueness of the optimality system are defined. The characterization of the optimal control gives rise to both the boundary and interior solutions, with the former indicating that the resource should be harvested if and only if the value of the net revenue per unit harvest (due to the application of up to the maximum fishing effort) is at least the value of the shadow price of fish stock. Numerical simulations with empirical data on the sardinella are carried out to validate the theoretical results.

Keywords: Optimal control, Compensation, Critical depensation, Bifurcation, Shadow price, Ghana sardinella fishery

1 Introduction

Fish stocks across the world are increasingly under pressure as a result of the excessive harvesting capacity prevalent in the fishing industry. Thus, it is common that abundant stocks may suddenly collapse. A review by Mullon et al. [1] of the FAO world fisheries data on catch for the past five decades showed that as much as 25% of fisheries' collapses occurred during that period. Thus, the prudent and effective management of fishery resources in order to ensure their sustainability for future generations cannot be overemphasized.

Various studies addressed the sustainable harvesting of renewable natural resources, especially fisheries [2-8]. Dubey and Patra [2] proposed and analyzed a dynamic model with crowding effect of a renewable resource that humans used for their nourishment. They obtained the optimal level of harvesting for the resource through the application of Pontryagin's maximum principle. The sustainable harvesting of prey species in a predator-prey model in the Sundarbans ecosystem was investigated by Hasan et al. [4]. They established the local and global stability of the model as well as obtaining the optimal harvesting strategy. Kar [5] explored a predator-prey system with a prey refuge that also included independent

harvesting of either species. The study showed that, with harvesting effort serving as a control, the system could be steered towards a desirable state, and so breaking its cyclic behavior. A two-predator one-prey system was analyzed and discussed by Pal et al. [6]. They focused on defining the sustainable yield of the resource while concurrently maintaining the ecological resilience of the system. Panja [7] developed and discussed a dynamical model involving the interactions of a prey, predator and scavenger species. The study revealed that harvesting of the predator can serve as a control mechanism for the chaotic behavior of the system. The optimal exploitation of a fishery under critical depensation was analyzed by Kar and Misra [8]. They addressed the stability properties and defined the optimal tax policy for the system.

However, the present study investigates the relative performance of both compensation and critical depensation models when subjected to harvesting. Therefore, an optimal control problem with quadratic revenues in the objective functional and a compensation model as the biological dynamics is analyzed. Moreover, another control problem with the biological dynamics representing a critical depensation model is tackled. It must be noted that, instead of the linear revenues in most resource problems, quadratic revenues are employed in

* Corresponding author e-mail: mibrahim@ucc.edu.gh

this study to account for diminishing returns whenever a bumper harvest occurs [9]. Another novelty of this study is the exploration of the relationship between the shadow price and the marginal net revenue as it relates to the optimal fishing effort. In Section Two, the optimal control problem is formulated comprising the biomass dynamics – compensation model – as well as the complete bioeconomic model. In addition, it covers the optimality of the model, which consists of the characterization of the optimal control, as well as the existence and uniqueness of the optimality system. An optimal control problem with a critical depensation model as biological dynamics is addressed in Section Three. Furthermore, bifurcation analysis of the model is explored and numerical simulations are conducted. Section Four is devoted to summary and conclusion.

2 Compensation Model

Let the generic biological model be given by

$$\frac{dx(t)}{dt} = g(x) - h(t), \quad (1)$$

where $x(t)$ represents the size of fish stock (or biomass) at time t , $g(x)$ is the net natural growth rate and $h(t)$ is the rate of harvest of stock at time t .

Models in which the per capita growth rate $\frac{g(x)}{x}$ is a decreasing function of the stock size are known as pure compensation models. They imply that, irrespective of how low the population is, it will always recover when fishing ceases [10]. A typical example of a compensation model is the logistic growth curve (see Figure 1 (a)). Thus, the Schaefer model [11] can be expressed as

$$\frac{dx(t)}{dt} = rx(t) \left(1 - \frac{x(t)}{K} \right) - qE(t)x(t), \quad x(0) = x_0, \quad (2)$$

where x_0 is the initial biomass level, r is the intrinsic growth rate of fish stock, q is the catchability coefficient, $E(t)$ is the rate of fishing effort at time t , and K denotes the carrying capacity of the ecosystem in the absence of harvesting. It is easily noted that the net growth rate of the logistic (without harvesting) is strictly concave and positive for $0 < x < K$ (see Figure 1 (b)). Moreover, the per capita growth rate decreases for $0 \leq x \leq K$.

Note that the harvest (or yield) is given by

$$h(t) = qE(t)x(t). \quad (3)$$

There are two hyperbolic equilibrium points associated with Eq. (2), namely 0 and a positive equilibrium point

$$x_{eqm} = K \left(1 - \frac{qE}{r} \right), \quad (4)$$

provided $E < \frac{r}{q}$.

The equilibrium point 0 is unstable while x_{eqm} is stable. Since these equilibrium points are hyperbolic, the dynamical system is structurally stable. It is instructive to note that the model undergoes a transcritical bifurcation at the point $E = \frac{r}{q}$. That is, there exists a single nonhyperbolic equilibrium point, 0, which makes the system structurally unstable. In other words, for any initial population x_0 , the resource will eventually go into extinction. When $E > \frac{r}{q}$, there is a single non-negative hyperbolic equilibrium point, 0. Of course, it is stable, and the system is structurally stable. Thus, for any initial population level, the resource will die out in finite time. For the sake of completeness, the other equilibrium point is $-x_{eqm}$, which is hyperbolic and unstable. For further details, see Ibrahim [12].

Incorporating economic parameters [9,13] into Eq. (2), the optimal control problem can be formulated as

$$\begin{aligned} \max_E J(E) &= \int_0^{\infty} e^{-\delta t} \left[p_1 q E x - \frac{p_2}{2} (q E x)^2 - c E \right] dt \\ \text{subject to } \frac{dx}{dt} &= r x \left(1 - \frac{x}{K} \right) - q E x \quad (5) \\ x(0) &= x_0 \\ 0 \leq E &\leq E_{max}, \end{aligned}$$

where δ is the annual discount rate, p_1 is the price of landed fish, p_2 represents the price component of the term involving diminishing returns when there is a huge quantity of fish on sale, c represents the cost per unit of fishing effort and E_{max} is the maximum allowable fishing effort.

The biological and inflation-adjusted economic parameter values used for the study are presented in Table 1.

The linear and quadratic revenues are depicted in Figure 2. The diminishing returns on the linear revenues are such that when the fishing effort and biomass are at the maximum sustainable yield (MSY) reference point, the quadratic gross revenues are 15% less than the linear revenues. Therefore, p_2 is computed as

$$\begin{aligned} p_2 &= \frac{0.30 p_1}{q E_{MSY} x_{MSY}} \\ &= \$5.07 \times 10^{-4} \text{ year / tonne}^2. \end{aligned}$$

Data on the static reference points, maximum economic yield (MEY), binomic equilibrium (BE) and the MSY are presented in Table 2. It shows that, at the MEY levels, the maximum revenue and the highest stock size are attained. Thus, apart from providing the most revenue, it is also the most conservationist among the three. Clearly, the level at MSY provides the highest yield, and at the BE level, it provides the most effort, lowest stock size, lowest yield, and of course, zero revenue. Thus, fisheries managers must guard against this scenario.

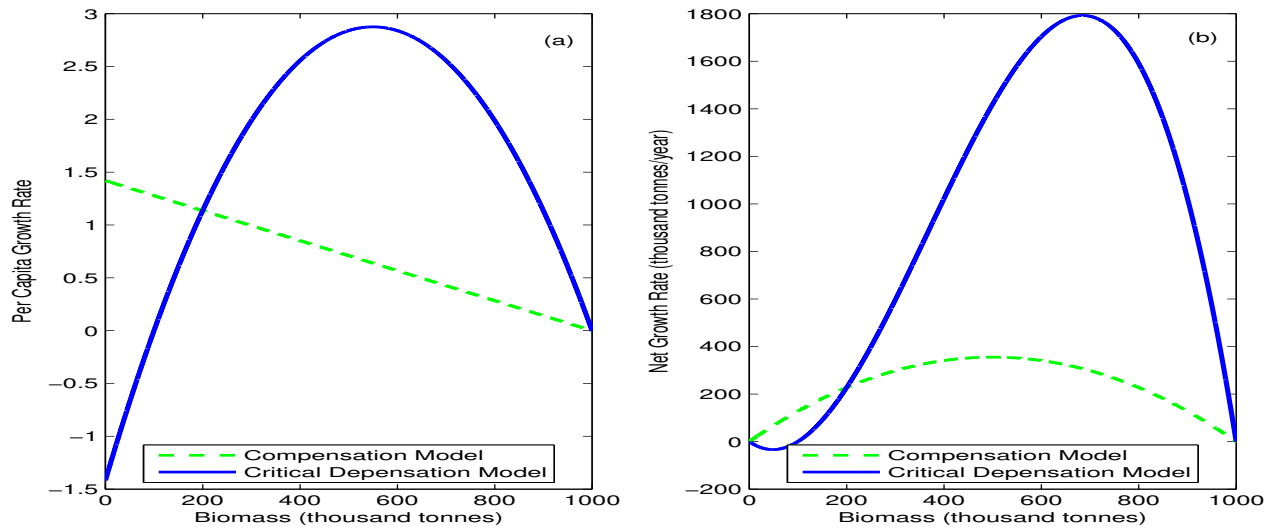


Fig. 1: Per capita growth rate and net growth rate for compensation and critical depensation models

Table 1: Parameter values for model

Parameter	Description	Value	Units	Source
δ	Discount rate	0.15	year ⁻¹	Estimated
q	Catchability coefficient	1.8×10^{-6}	trip ⁻¹ year ⁻¹	[14]
r	Intrinsic growth rate	1.42	year ⁻¹	[14]
K	Carrying capacity	1,000,000	tonnes	[14]
M	Critical biomass level	100,000	tonnes	Estimated
c	Cost per fishing trip	195	\$ trip ⁻¹ year ⁻¹	[14]
p_1	Ex-vessel price of fish	600	\$ tonne ⁻¹	[14]

Table 2: Annual net revenue at the static reference points

Reference point	MEY	MSY	BE
x	625,570	500,000	199,704
E	295,384	394,444	631,344
h	332,610	355,000	226,986
Sustainable net revenue (\$ year ⁻¹)	139,780,389	104,135,915	0

2.1 Optimality of the model

Sufficiency conditions for the model are investigated. In particular, the existence of an optimal control is defined. Also, the characterization of the optimal control and the existence and uniqueness of the optimality system are analyzed.

The goal, as stated in the objective functional, is to maximize the present-value of the net revenue. Thus, we seek an optimal control E^* such that

$$J(E^*) = \max\{J(E) \mid E \in U\},$$

where the control set is Lebesgue measurable for an infinite time horizon, and defined by

$$U = \{E \mid 0 \leq E(t) \leq E_{max}, t \in [0, \infty)\}.$$

As already intimated, in the solution of an optimal control problem, necessary and sufficient conditions of the problem need to be investigated and verified. Thus, conditions that are sufficient for the existence of an optimal control to the underlying problem (5) are examined. To this end, a sufficiency result proposed by Fleming and Rishel [15] is invoked.

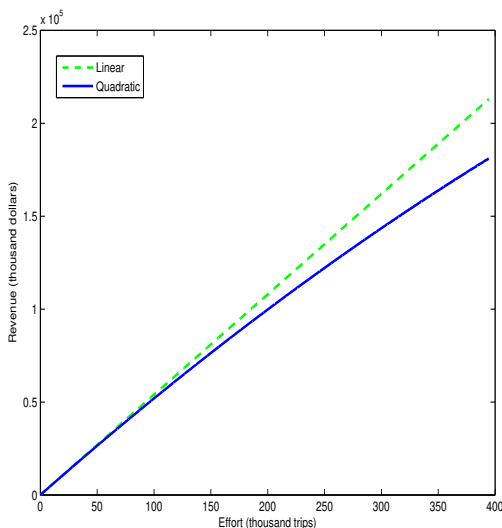


Fig. 2: Linear and quadratic revenues

Theorem 2.1. Let U be the control set. Then there exists an optimal control E^* in U that maximizes the objective functional $J(E)$ if the following conditions hold:

- (i) The class of all initial conditions with a control E in U together with the state equation is nonempty.
- (ii) The control set U is closed and convex.
- (iii) The right hand side of the state system is bounded by a function linear in the state and control variables.
- (iv) The integrand of $J(E)$ is concave on U .
- (v) There exist constants $w_1, w_2 > 0$ and $\eta > 1$ such that the integrand is bounded above by $w_1 - w_2E^\eta$.

Proof. To verify the first condition, the Picard-Lindelof existence theorem [16] guarantees the existence and uniqueness of a solution to a state equation with bounded coefficients.

For verification of condition 2, by definition, the control set U is closed and convex. In order to verify condition 3: first, the boundedness of the solution to the state equation is defined using the comparison theory of differential equations and the theorem on differential inequalities. Since

$$x' = rx \left(1 - \frac{x}{K}\right) - qEx \leq rx \left(1 - \frac{x}{K}\right)$$

for $0 \leq t < \infty$ and $x_0 > 0$, then

$$x' \leq rx \left(1 - \frac{x}{K}\right).$$

Thus,

$$x(t) \leq \frac{x_0 K}{x_0 + (K - x_0)e^{-rt}}.$$

Therefore, as $t \rightarrow \infty$,

$$0 \leq x \leq K.$$

Second, the right hand side of the state equation can be written as

$$S(t, x, E) = rx \left(1 - \frac{x}{K}\right) - qEx \leq rx \leq rK.$$

Hence the bound on the right hand side is given by

$$S(t, x, E) \leq rK.$$

The next task is to prove that the integrand of the objective functional, $f(t, x, E) = e^{-\delta t} L(t, x, E) = e^{-\delta t} [p_1 qEx - \frac{p_2}{2} (qEx)^2 - cE]$ is concave on U . Thus, the goal is to show that, for $0 \leq m \leq 1$,

$$mf(t, x, E_1) + (1 - m)f(t, x, E_2) \leq f(t, x, mE_1 + (1 - m)E_2),$$

or

$$mL(t, x, E_1) + (1 - m)L(t, x, E_2) \leq L(t, x, mE_1 + (1 - m)E_2).$$

The proof is commenced by noting that the difference of $mL(t, x, E_1) + (1 - m)L(t, x, E_2)$ and $L(t, x, mE_1 + (1 - m)E_2)$ is given by

$$\begin{aligned} & mL(t, x, E_1) + (1 - m)L(t, x, E_2) - L(t, x, mE_1 + (1 - m)E_2) \\ &= mp_1 qE_1 x - m \frac{p_2}{2} (qE_1 x)^2 - mcE_1 + (1 - m)p_1 qE_2 x \\ &- (1 - m) \frac{p_2}{2} (qE_2 x)^2 - (1 - m)cE_2 - p_1 qx[mE_1 + (1 - m)E_2] \\ &+ \frac{p_2}{2} (qx)^2 [mE_1 + (1 - m)E_2]^2 + c[mE_1 + (1 - m)E_2]. \end{aligned}$$

The simplification of the right-hand-side gives

$$-\frac{p_2}{2} q^2 x^2 (m - m^2) (E_1 - E_2)^2 \leq 0,$$

since

$$(m - m^2) \geq 0 \text{ for } 0 \leq m \leq 1.$$

Hence

$$mL(t, x, E_1) + (1 - m)L(t, x, E_2) \leq L(t, x, mE_1 + (1 - m)E_2).$$

This satisfies condition 4.

Finally, to verify condition 5, it is noted that x and E are bounded. Thus, there exists a $D > 0$ such that $x \leq D$ and $E \leq D$ on $[0, \infty)$, where $D = \max(K, E_{max})$. Moreover, choose $B > 0$ to be a minimum value of x . Then

$$\begin{aligned} p_1 qEx - \frac{p_2}{2} (qEx)^2 - cE &\leq p_1 qD^2 - \frac{p_2}{2} q^2 B^2 E^2 \\ &\leq w_1 - w_2 E^2, \end{aligned}$$

where

$$w_1 = p_1 qD^2, \quad w_2 = \frac{p_2}{2} q^2 B^2 \quad \text{and} \quad \eta = 2.$$

This completes the proof. \square

Additionally, let $w_1 - w_2E^2 = G$. Then

$$\int_0^\infty e^{-\delta t} \left[p_1 q E x - \frac{p_2}{2} (q E x)^2 - c E \right] dt \leq \int_0^\infty e^{-\delta t} G dt = \frac{G}{\delta}.$$

Hence the objective functional is convergent as $t \rightarrow \infty$.

The characterization of the optimal control involves obtaining an explicit formulation for the optimal control level. Since the existence of an optimal control to Problem (5) has already been established, a version of Pontryagin's maximum principle (Pontryagin et al. [17]) is employed.

Theorem 2.2. For an optimal control E^* and an accompanying solution to the state equation, there exists an adjoint variable λ satisfying

$$\lambda' = \left(\delta - r + \frac{2rx}{K} \right) \lambda - (p_1 - p_2 q E x - \lambda) q E \quad (6)$$

and the transversality condition,

$$\lim_{t \rightarrow \infty} \lambda(t) = 0.$$

In addition, E^* can be presented as

$$E^* = \min \left(E_{max}, \left(\frac{(p_1 - \lambda) q x - c}{p_2 q^2 x^2} \right)^+ \right).$$

Proof. The current-value Hamiltonian for the optimal control problem (5) is

$$H = p_1 q E x - \frac{p_2}{2} (q E x)^2 - c E + \lambda \left[r x \left(1 - \frac{x}{K} \right) - q E x \right]. \quad (7)$$

Therefore, we obtain Eq. (6) from the adjoint equation

$$\lambda' = \delta \lambda - \frac{\partial H}{\partial x}.$$

The optimality condition is given by

$$\frac{\partial H}{\partial E} = p_1 q x - p_2 q^2 E x^2 - c - \lambda q x = 0.$$

Thus,

$$E^* = \frac{(p_1 - \lambda) q x - c}{p_2 q^2 x^2}. \quad (8)$$

The characterization of the optimal control is

$$\begin{cases} E^* = 0 & \text{if } \frac{\partial H}{\partial E} < 0, \\ 0 \leq E^* \leq E_{max} & \text{if } \frac{\partial H}{\partial E} = 0, \\ E^* = E_{max} & \text{if } \frac{\partial H}{\partial E} > 0. \end{cases}$$

Employing standard arguments regarding the bounds on the control, the optimal control E^* is given by

$$\begin{cases} 0 & \text{if } \lambda > p_1 - \frac{c}{q x}, \\ \frac{(p_1 - \lambda) q x - c}{p_2 q^2 x^2} & \text{if } p_1 - \frac{(c + p_2 q^2 x^2 E_{max})}{q x} \leq \lambda \leq p_1 - \frac{c}{q x}, \\ E_{max} & \text{if } \lambda < p_1 - \frac{(c + p_2 q^2 x^2 E_{max})}{q x}. \end{cases} \quad (9)$$

This implies that the optimal control comprises both the boundary solutions (or binding constraints) and the interior solution. The boundary solutions indicate that the resource should be harvested if and only if the marginal net revenue of harvest as a result of application of up to the maximum level of fishing effort exceeds the current-value shadow price of the resource.

In compact notation,

$$E^* = \min \left(E_{max}, \left(\frac{(p_1 - \lambda) q x - c}{p_2 q^2 x^2} \right)^+ \right).$$

The optimality system comprises the state equation, the adjoint equation, the initial and transversality conditions together with the characterization of the optimal control. Therefore,

$$x' = r x \left(1 - \frac{x}{K} \right) - \min \left(E_{max}, \left(\frac{(p_1 - \lambda) q x - c}{p_2 q^2 x^2} \right)^+ \right) q x,$$

$$\begin{aligned} \lambda' &= \left(\delta - r + \frac{2rx}{K} \right) \lambda \\ &- \left(p_1 - p_2 \min \left(E_{max}, \left(\frac{(p_1 - \lambda) q x - c}{p_2 q^2 x^2} \right)^+ \right) \right) q x - \lambda \\ &\times \min \left(E_{max}, \left(\frac{(p_1 - \lambda) q x - c}{p_2 q^2 x^2} \right)^+ \right) q, \end{aligned}$$

$$\text{with } x(0) = x_0 \text{ and } \lim_{t \rightarrow \infty} \lambda(t) = 0.$$

Thus, the proof has been completed. \square

It must be noted that if the state trajectories are bounded, it is sufficient for the transversality condition to become $\lim_{t \rightarrow \infty} \lambda(t) = 0$ [18, 19].

The existence of the optimal control has already been established by Theorem 2.1. Next, uniqueness of the optimal control is defined. Given that the state and adjoint equations are a priori bounded, and the state equation is continuously differentiable, then through the application of the mean value theorem, the state equation satisfies the Lipschitz condition with regard to the state variable. Thus, the uniqueness of the optimality system for small time intervals is guaranteed [20].

2.2 Numerical simulations

To achieve the stated objectives of the study, the optimality system is implemented using an iterative method involving the Runge-Kutta Fourth Order scheme. This involves the Forward-Backward Sweep method [20], where the state equation is solved forward in time and the adjoint equation is solved backward in time until convergence (if any) is achieved.

The maximum fishing effort is initially set at the BE level, E_{BE} , and subsequently, at the MEY and MSY levels. First, the model is simulated for a fixed rate of

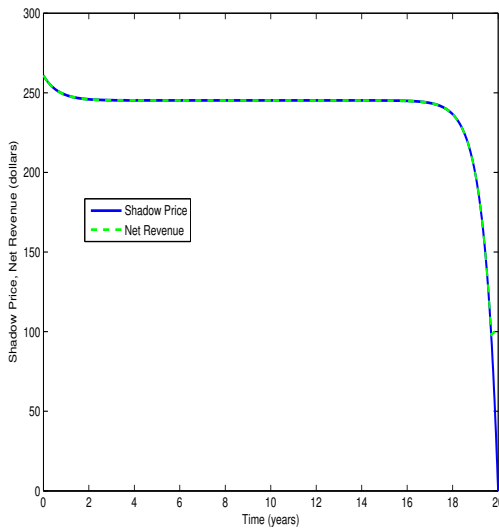


Fig. 3: Shadow price and net revenue for $E_{max} = 631,344$, $x_0 = 550,000$ and $T = 20$

fishing effort while varying the initial biomass level to determine the long-run dynamics. Second, simulations are carried out with a fixed initial biomass level while varying the rate of fishing effort. Third, the initial stock level is set very low while harvesting at the MSY level in order to test the compensatory properties of the model.

The long-run scenario, as shown in Figure 3, depicts fishing at a maximum effort rate of 631,344 trips (BE effort rate), $x_0 = 550,000$ tonnes and $T = 20$ years. At the beginning of the harvesting process, the shadow price and marginal net revenue appear to intersect at US \$260.94. This signifies that the revenue as a result of an extra tonne of fish added to the biomass is exactly equal to the expected revenue from harvesting the fish. Hence, at this stage, it is beneficial to harvest, but not at the maximum effort rate. As time progresses, the shadow price and net revenue reduce and then remain constant for the majority of the time horizon. Subsequently, the shadow price experiences a sharp fall down to zero at the final time horizon, $T = 20$ years. On the other hand, the net revenue ends at US \$100.46. The optimal control alternates between the interior and boundary controls. This shows that for a long-term time horizon (or under equilibrium conditions), it is not optimal to exert the full maximum effort for the entire horizon (see Figure 4).

Simulation results for the effort level and stock size relating to the case where $E_{max} = 631,344$ trips and $T = 20$ years are presented in Figure 4. In the effort plot, it is observed that when the maximum effort level E_{max} is set at the BE level, the optimal effort levels appear to initially follow different paths, starting from around 283,108 trips and 378,192 trips respectively for $x_0 = 550,000$ tonnes and $x_0 = 750,000$ tonnes. Thereafter, the effort levels converge at about 381,200

trips, before rising and ending at almost 631,344 trips at the final horizon. Furthermore, the fish biomass levels initially follow different trajectories before converging at 596,500 tonnes for a majority of the time horizon. Afterwards, the biomass decreases for both initial values to a common value of around 431,274 tonnes (see biomass plot).

Assuming an initial population size of 550,000 tonnes, the total net revenue over the twenty-year horizon corresponding to the given level of harvesting is computed as US \$707,480,000. The net revenue for $x_0 = 750,000$ tonnes is US \$753,090,000, an increase of 6%.

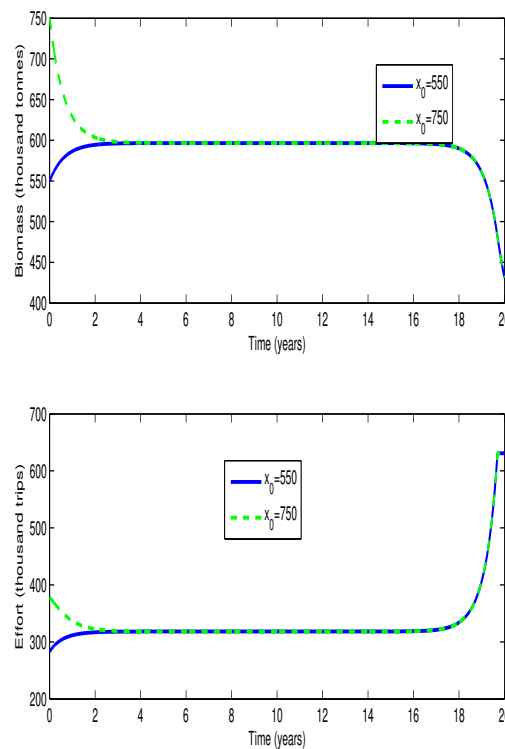


Fig. 4: Effort and biomass levels for $x_0 = 550,000$; 750,000, $E_{max} = 631,344$ and $T = 20$

When the rate of fishing effort is pegged at the BE level, the iterates still converge. This is a result of the maximum effort level, 631,344 trips being less the bifurcation point of the model, 788,889 trips. Moreover, for the majority of the time horizon, the optimal effort level is at most about 381,200 trips. This is far less than the maximum effort set at the BE level.

Figure 5 depicts fishing at a maximum effort rate of 295,384 trips, $x_0 = 550,000$ tonnes and $T = 20$ years. When harvesting commences, the shadow price and marginal net revenue start at about US \$254.91. However, at the final time horizon, the net revenue increases to US

\$258,23 while the shadow price reduces to zero. This shows that for a long-term time horizon (or under equilibrium conditions), it is optimal to exert up to the maximum effort, as the revenue curve is always on or above the shadow price curve.

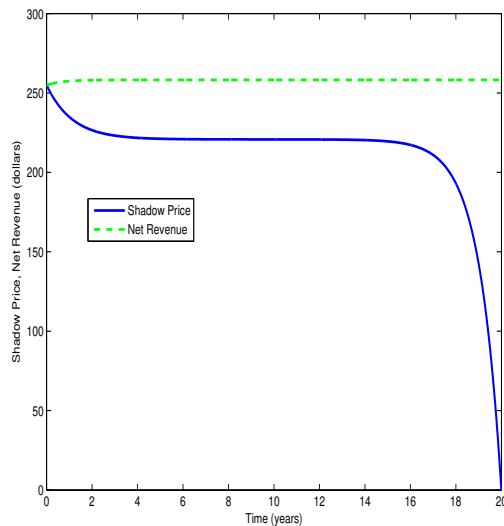


Fig. 5: Shadow price and net revenue for $E_{max} = 295,384$, $x_0 = 550,000$ and $T = 20$

The harvest level and stock size relating to the case where $x_0 = 550,000$ tonnes, $E_{max} = 295,384$ trips and $E_{max} = 394,444$ trips are presented in Figure 6. It is observed that when the maximum effort level E_{max} is set at the MEY and MSY levels, the optimal effort level follows different paths. The effort level for MEY is around the equilibrium value of 295,384 trips throughout the twenty-year horizon. On the other hand, the effort level for MSY starts at a lower value of 283,129 trips and rises to 318,297 trips for the majority of the time horizon. It eventually rises again before ending at nearly the maximum value, 394,444 trips. Furthermore, the fish biomass levels follow different trajectories. The biomass increases for effort level at MEY to its equilibrium value of approximately 625,752 tonnes. For the effort level at MSY, the biomass increases to 596,716 tonnes for the majority of the time horizon before finally decreasing to 525,111 tonnes. Given an initial population size of 550,000 tonnes, the total net revenue over the twenty-year horizon corresponding to the harvest levels at MEY and MSY are computed as US \$703,830,000 and US \$707,270,000 respectively. The net revenue at MSY is about 1% greater than the revenue at MEY.

In Figure 7, when the maximum effort level E_{max} is set at the MSY level, the optimal effort level initially indicates no fishing for either of the initial biomass levels. Afterwards, with harvesting starting a fraction early for the higher initial biomass level, both effort rates stabilize

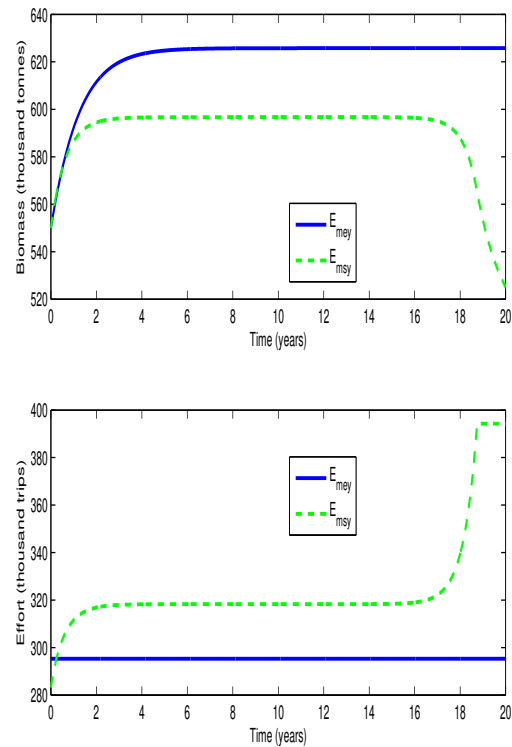


Fig. 6: Effort and biomass levels for $x_0 = 550,000$, $E_{max} = 295,384$; 394,444 and $T = 20$

to around 320,00 trips, before a slight increase to the equilibrium value of 394,444 trips at the end of the horizon. With respect to the stock size, there is positive convergence for both initial biomass levels to around 600,000 tonnes, before a slight decrease to 525,000 tonnes at the end. This agrees with the theoretical assertions about the compensation model: regardless the level of stock size, the population will always recover. The net revenues for $x_0 = 90,000$ and $x_0 = 110,000$ tonnes are US \$536,400,000 and US \$550,070,000 respectively; a difference of 6%.

3 Critical Depensation Model

In depensation models, the per capita growth rate is an increasing function of stock size for small values of x , representing low (or depleted) stock levels. Depensation models with a critical biomass level below which the population fails to recover even after the cessation of fishing are known as critical depensation models. The modified logistic with critical depensation (or Allee effect) is the typical model employed for depensation studies [8, 21]. Therefore, the critical depensation model

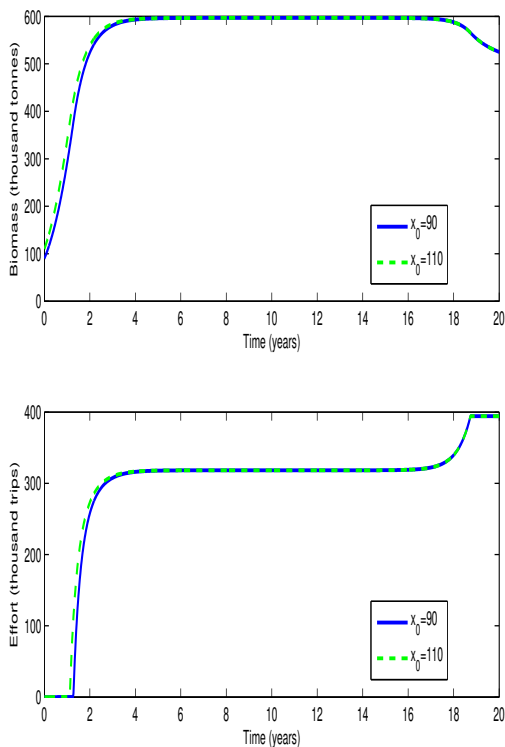


Fig. 7: Effort and biomass levels for $x_0 = 90,000; 110,000$
 $E_{max} = 1,454,477$ and $T = 10$

with harvesting is given by

$$\frac{dx(t)}{dt} = rx(t) \left(1 - \frac{x(t)}{K} \right) \left(\frac{x(t)}{M} - 1 \right) - qE(t)x(t), \quad x(0) = x_0, \tag{10}$$

where the sustainable population threshold M is called the minimum viable population (MVP) level [10]. The net growth rate for the model (without harvesting) is strictly convex and negative for $0 < x < M$, convex and positive for $M < x < \frac{1}{3}(K + M)$, and concave and positive for $\frac{1}{3}(K + M) \leq x < K$. Of course, the equilibrium points of the unharvested model are 0, M and K . Also, $x = \frac{1}{3}(K + M)$ is a point of inflection for the unharvested model; see Figure 1 (b). Furthermore, the per capita growth rate of the unharvested model is increasing for $0 \leq x \leq \frac{1}{2}(K + M)$ and decreasing for $\frac{1}{2}(K + M) < x \leq K$ (see Figure 1 (a)).

There are three hyperbolic equilibrium points associated with Eq. (10). They are 0 and two positive equilibrium points:

$$x_1 = \frac{1}{2} \left[(K + M) - \sqrt{(K - M)^2 - \frac{4qEKM}{r}} \right], \quad \text{and} \tag{11}$$

$$x_2 = \frac{1}{2} \left[(K + M) + \sqrt{(K - M)^2 - \frac{4qEKM}{r}} \right], \tag{12}$$

provided $E < \frac{1}{4} \frac{r(K - M)^2}{qKM}$.

When $E = \frac{1}{4} \frac{r(K - M)^2}{qKM}$, there are two equilibrium points: 0 and

$$x_1 = x_2 = \frac{1}{2}(K + M). \tag{13}$$

Therefore, $E = \frac{1}{4} \frac{r(K - M)^2}{qKM}$ is a saddle-node bifurcation point for the model.

Moreover, when $E > \frac{1}{4} \frac{r(K - M)^2}{qKM}$, there is only a single real equilibrium point: 0.

Theoretically, the MSY is the maximum yield that can be sustained indefinitely. Therefore, from Eq. (10), the sustainable yield is given by

$$h_S = qEx = rx \left(1 - \frac{x}{K} \right) \left(\frac{x}{M} - 1 \right). \tag{14}$$

The MSY occurs when

$$\frac{dh_S}{dx} = \frac{-3r}{KM}x^2 + \frac{2r}{KM}(K + M)x - r = 0. \tag{15}$$

Thus,

$$x = \frac{1}{3} \left[(K + M) \pm \sqrt{K^2 - KM + M^2} \right].$$

So

$$x_{MSY} = \frac{1}{3} \left[(K + M) + \sqrt{K^2 - KM + M^2} \right].$$

and

$$E_{MSY} = \frac{r}{9qKM} \left[K^2 - 4K + M^2 + (K + M)\sqrt{K^2 - KM + M^2} \right].$$

Thus,

$$h_{MSY} = qE_{MSY}x_{MSY}.$$

Incorporating economic parameters into Eq. (10), the optimal control problem with critical depensation can be presented as

$$\begin{aligned} \max_E J(E) &= \int_0^\infty e^{-\delta t} \left[p_1 qEx - \frac{p_2}{2} (qEx)^2 - cE \right] dt \\ \text{subject to } \frac{dx}{dt} &= rx \left(1 - \frac{x}{K} \right) \left(\frac{x}{M} - 1 \right) - qEx \tag{16} \\ x(0) &= x_0 \\ 0 &\leq E \leq E_{max}. \end{aligned}$$

3.1 Bifurcation analysis

Bifurcation in a dynamical system is concerned about the number of equilibrium points and their stability properties when a key parameter is varied [12]. The solution curves

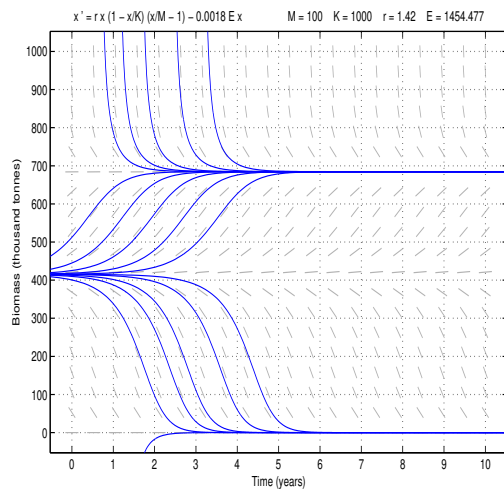


Fig. 8: Solution curves for $E = 1,454,477$

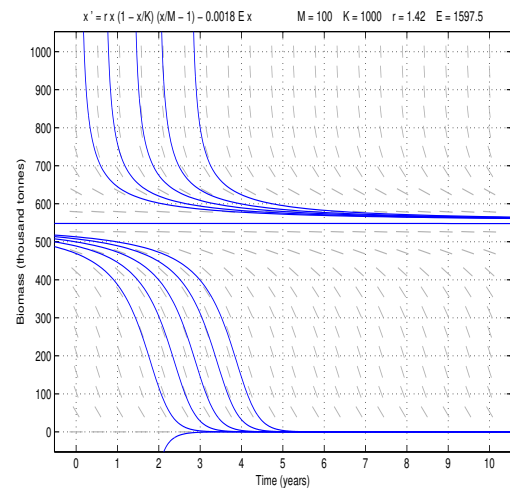


Fig. 9: Solution curves for $E = 1,597,500$

for the various scenarios depicting the effects of a variation in the fishing effort on the stock size are presented.

Solution curves reflecting the scenario where $E = E_{MSY} = 1,454,477$ trips are presented in Figure 8. It can be observed that there are three hyperbolic equilibrium points: 0 , $x_1 = 415,354$ tonnes and $x_2 = 684,646$ tonnes. For any initial biomass level $x_0 > x_2$, the population approaches the equilibrium population, x_2 in the long run. Similarly, for $x_1 < x_0 < x_2$, the population asymptotically approaches x_2 ; whereas for $0 < x_0 < x_1$, the population asymptotically approaches 0 . Thus, the biomass levels 0 and x_2 are stable while x_1 is unstable. Since all the equilibrium points are hyperbolic, the dynamical system is structurally stable. Of course, biomass levels starting from the equilibrium levels; 0 , x_1 and x_2 remain there indefinitely.

In Figure 9, solution curves corresponding to the case where $E = 1,597,500$ trips, the bifurcation point, are presented. At the bifurcation point, there are two equilibrium points: 0 and $x_{bf} = 550,000$ tonnes. For any initial biomass level $x_0 > x_{bf}$, the population approaches x_{bf} in the long run. However, for $0 < x_0 < x_{bf}$, the population asymptotically approaches 0 . Thus, at the saddle-node bifurcation point, the equilibrium point x_{bf} is nonhyperbolic and semi-stable (making the system structurally unstable). However, the equilibrium point 0 is hyperbolic and stable. Clearly, biomass levels starting from the equilibrium levels 0 and x_{bf} remain there indefinitely. Hence, for a given initial biomass level, the long-term population of fish stock is towards extinction if $x_0 < 550,000$ tonnes.

The case where effort level, $E = 1,740,523$ trips, is greater than the bifurcation point is shown in Figure 10. For any initial biomass level $x_0 > 0$, the population approaches the hyperbolic equilibrium population 0 in finite time. Thus, corresponding to this effort level, there

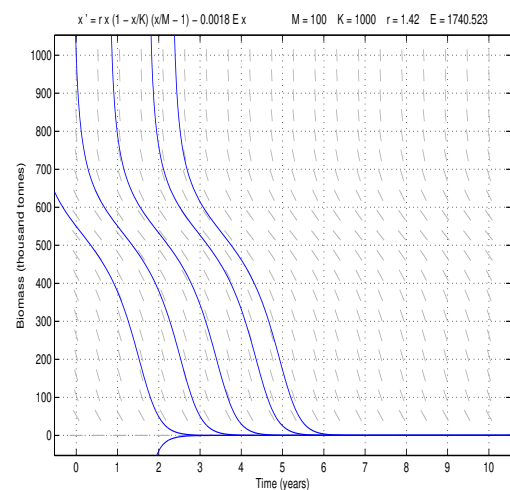


Fig. 10: Solution curves for $E = 1,740,523$

exists a nonnegative equilibrium biomass level, 0 which is stable (making the system structurally stable). Hence, in this situation, whatever the initial fish population, the fish will die out as a result of overfishing (or excessive harvesting) in finite time.

3.2 Optimality of the model

With reference to the background information presented in Section 2.1, there exists an optimal control E^* for the optimal control problem (16) that maximizes the objective functional over the control set. In addition, the optimality system for the control problem is unique based on the arguments espoused in the afore-mentioned section.

Theorem 3.1. For an optimal control E^* and an accompanying solution to the state equation, there exists an adjoint variable λ satisfying

$$\lambda' = (p_2qEx - p_1)qE + \lambda \left[\frac{3r}{KM}x^2 - \frac{2r}{KM}(K + M)x + qE + r + \delta \right] \tag{17}$$

and the transversality condition,

$$\lim_{t \rightarrow \infty} \lambda(t) = 0.$$

In addition, E^* can be expressed as

$$E^* = \min \left(E_{max}, \left(\frac{(p_1 - \lambda)qx - c}{p_2q^2x^2} \right)^+ \right).$$

Proof. The current-value Hamiltonian for the optimal control problem (16) is

$$H = p_1qEx - \frac{p_2}{2}(qEx)^2 - cE + \lambda \left[rx \left(1 - \frac{x}{K} \right) \left(\frac{x}{M} - 1 \right) - qEx \right]. \tag{18}$$

Therefore, Eq. (17) can be obtained from the adjoint equation

$$\lambda' = \delta\lambda - \frac{\partial H}{\partial x}.$$

The optimality condition is given by

$$\frac{\partial H}{\partial E} = p_1qx - p_2q^2Ex^2 - c - \lambda qx = 0.$$

Thus,

$$E^* = \frac{(p_1 - \lambda)qx - c}{p_2q^2x^2}. \tag{19}$$

Therefore, E^* can be expressed as

$$\begin{cases} 0 & \text{if } \lambda > p_1 - \frac{c}{qx}, \\ \frac{(p_1 - \lambda)qx - c}{p_2q^2x^2} & \text{if } p_1 - \frac{(c + p_2q^2x^2E_{max})}{qx} \leq \lambda \leq p_1 - \frac{c}{qx}, \\ E_{max} & \text{if } \lambda < p_1 - \frac{(c + p_2q^2x^2E_{max})}{qx}. \end{cases} \tag{20}$$

This marks the end of the proof. \square

3.3 Numerical simulations

In Figure 11, fishing at a maximum effort rate of 1,454,477 trips (MSY effort rate), $x_0 = 200,000$ tonnes and $T = 10$ years, the shadow price and marginal net revenue start at US \$925.41 and US \$58.32 respectively. Thereafter, they intersect at about US \$272.77 signifying the start of harvesting of the resource. With time, both the shadow price and marginal revenue converge to US \$14.05 before ending at zero at the final horizon. Thus, it is optimal to harvest the resource, but not at the maximum available rate (see Figure 12).

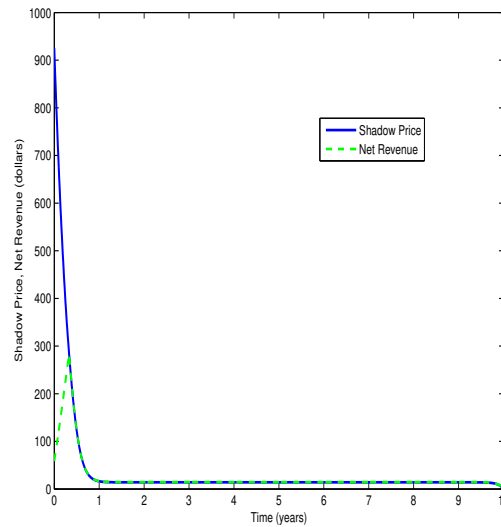


Fig. 11: Shadow price and net revenue for $E_{max} = 1,454,477$, $x_0 = 200,000$ and $T = 10$

It is observed in Figure 12 that when the maximum effort level E_{max} is set at the MSY level, the optimal effort levels initially follow different paths, starting from zero and 608,741 trips respectively for $x_0 = 200,000$ tonnes and $x_0 = 500,000$ tonnes. Over time, they converge at about 559,433 trips for the majority of the time horizon. Notice that there is a slight increase to 577,102 trips at the end of the horizon. In addition, the biomass levels initially follow different trajectories before converging to 912,812 tonnes for the remainder of the time horizon. For an initial population size of 200,000 tonnes, the total net revenue over the ten-year horizon corresponding to the given rate of harvesting is computed as US \$1,063,100,000. The net revenue for $x_0 = 500,000$ tonnes is US \$1,163,000,000, an increase of 9%.

Figure 13 depicts the scenario where the initial biomass level is fixed and the rate of harvesting varied. When the initial biomass level x_0 is set at 20% of the carrying capacity and the effort rate at the E_{MSY} and twice the E_{MSY} levels, the optimal effort rates as well as the biomass levels are identical. This means a 100% increase in the rate of harvesting has apparently no effect on the optimal effort and biomass levels. Consequently, the total net revenue over the ten-year horizon for both rates of harvesting is US \$1,063,100,000.

In Figure 14, when the initial biomass level is set at 100,000 tonnes (MVP level), the shadow price maintains a constant value of zero for the entire horizon. Similarly, the marginal net is also constant for the entire horizon, albeit at a much lower value of US \$-483.33. The implication is that no harvesting should take place for the entire horizon since the shadow price exceeds the net revenue. This outcome is not surprising, given that the

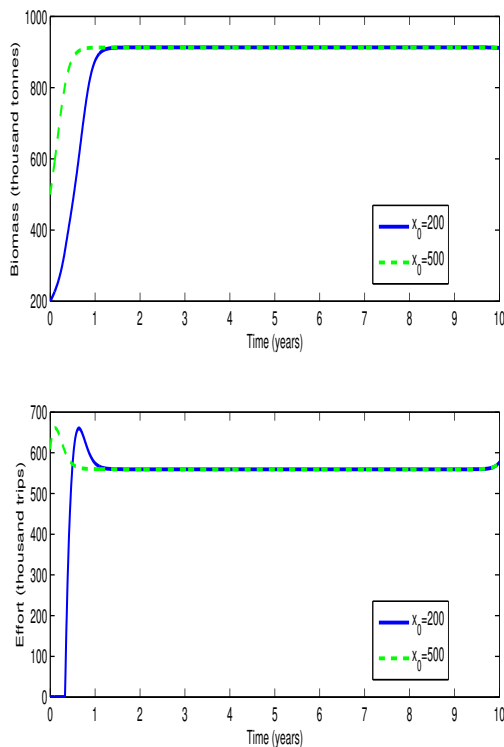


Fig. 12: Effort and biomass levels for $x_0 = 200,000; 500,000$ $E_{max} = 1,454,477$ and $T = 10$

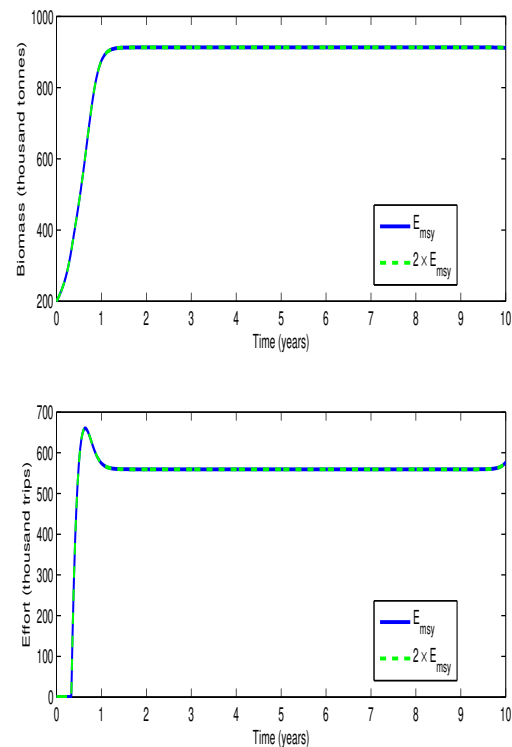


Fig. 13: Effort and biomass levels for $x_0 = 200,000, E_{max} = 1,454,477; 2,908,954$ and $T = 10$

initial stock size is at the minimum sustainable level for the resource.

Figure 15 manifests the situation where the initial biomass level x_0 is set at 10% of the carrying capacity and the effort rate at zero and E_{MSY} levels. The optimal effort rates as well as the biomass levels are identical. It implies that at the MVP level, it is not optimal to engage in any harvesting of the resource. Obviously, the total net revenue over the ten-year horizon for both rates of harvesting is zero.

Figure 16 exhibits that when the maximum effort level E_{max} is set at the MSY level, the optimal effort levels initially follow the same path, starting from zero trips for the respective initial biomass levels. Afterwards, the effort rate corresponding to $x_0 = 110,000$ tonnes converges to 559.443 trips, before a slight increase to 577,102 trips at the end of the horizon. However, the effort rate of $x_0 = 90,000$ tonnes remains at zero for the entire horizon. Regarding the stock size, there is positive convergence for the initial biomass level $x_0 = 110,000$ tonnes, while the stock is completely depleted in about six years for the case of initial biomass level $x_0 = 90,000$ tonnes. Stock will collapse for $x_0 = 90,000$ tonnes even when fishing ceases. This is in agreement with the analytic findings. The net revenue for $x_0 = 110,000$ tonnes is US \$799,420,000.

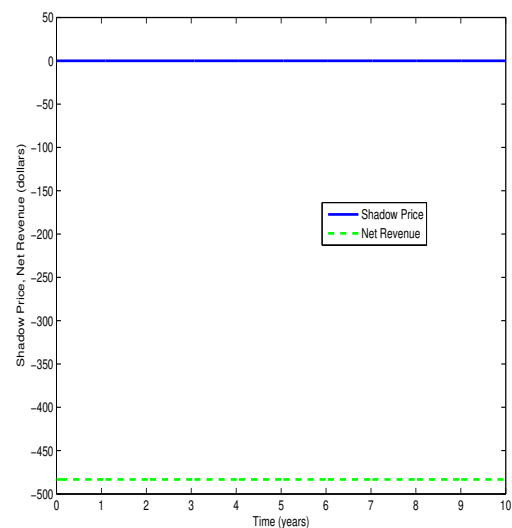


Fig. 14: Shadow price and net revenue for $E_{max} = 1,454,477, x_0 = 100,000$ and $T = 10$

4 Conclusions

The present research has addressed the determination of optimal fishing effort strategies for a fishery utilizing both

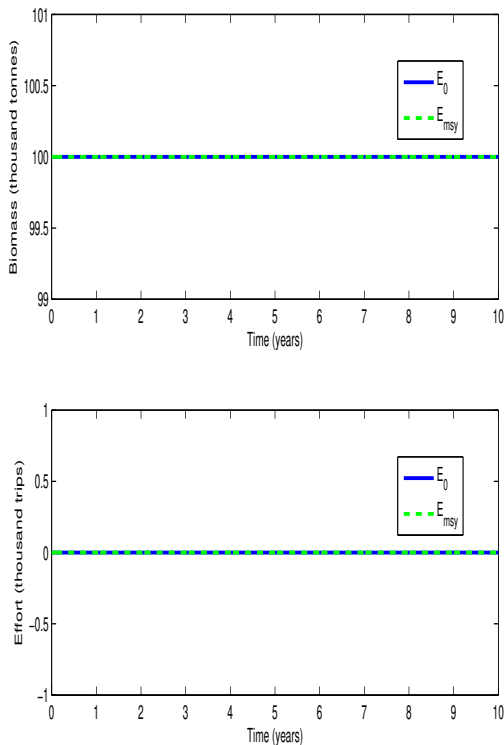


Fig. 15: Effort and biomass levels for $x_0 = 100,000$, $E_{max} = 0$; $1,454,477$ and $T = 10$

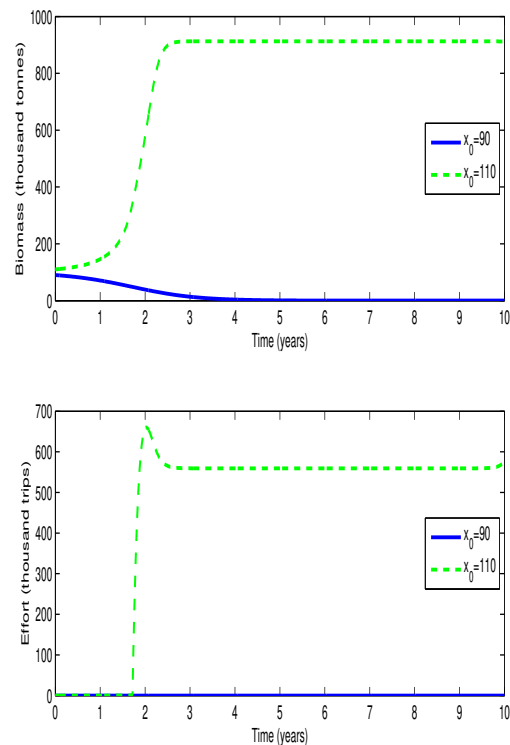


Fig. 16: Effort and biomass levels for $x_0 = 90,000$; $110,000$ $E_{max} = 1,454,477$ and $T = 10$

a compensation model and a critical depensation model. Bifurcation analyses on the models were conducted to ascertain stability properties of the equilibrium points. In addition, the objective functional of the canonical Gordon-Schaefer model was subjected to a modification. Instead of the typical linear revenues in the model, a more realistic revenue option – quadratic revenues – was considered. The analyses revealed that while the compensation model undergoes a transcritical bifurcation, the critical depensation model undergoes a saddle-node bifurcation. The existence of an optimal control for both models and the characterization of the control using Pontryagin's maximum principle were proved. Uniqueness of the optimality system is guaranteed due to the Lipschitz property of the models.

Numerical simulations were carried out on the models to find out the roles compensation and depensation play in the sustainable management of a fishery. For the compensation model, it was found to attain equilibrium status when the rate of harvesting is set at the MEY level. The model was also found to converge at both the MSY and BE levels. However, at these effort levels, the optimal control is mostly at the interior as opposed to the boundary (signifying harvesting, but not at the maximum level). For this model, the fishery always recovers, even at very low stock levels in the presence of harvesting. Meanwhile, the critical depensation model also converges

when the initial stock size is greater than the MVP level. However, for this model, very low initial biomass levels lead to cessation of fishing, at least for a portion of the time horizon. When the initial stock size is at the MVP level, it is not optimal to exert any fishing effort for the entire horizon; and when the stock size is below the MVP level, the fishery collapses with or without fishing. Therefore, to ensure sustainability of the resource, fishery managers should periodically monitor the stock to ensure that it is not depleted to levels beyond recovery. It is also important to note that the effort rate that produces the MSY for the critical depensation model is over 300% greater than that of the corresponding effort rate for the compensation model (assuming an MVP level of 10% of the carrying capacity).

Acknowledgement

The author is strongly grateful to the anonymous referees and Editor-in-Chief for their insightful comments and constructive suggestions.

References

- [1] C. Mullon, P. Freon, and P. Curry, The dynamics of collapse in world fisheries, *Fish and Fisheries*, **6**, 111-120 (2005).

- [2] A. Dubey and A. Patra, A mathematical model for optimal management and utilization of a renewable resource by population, *Journal of Mathematics*, **2013**, Article ID 613706, 1-9 (2013).
- [3] A. Dubey and A. Patra, Dynamics of phytoplankton, zooplankton and fishery resource model, *Applications and Applied Mathematics*, **9**, 217-245 (2014).
- [4] M. Z. Hasan, M. H. A. Biswas, and M. S. Uddin, A mathematical model for fish management in the Sundarbans ecosystem, *Open Journal of Mathematical Analysis*, **3**, 42-49 (2019).
- [5] T. K. Kar, Modelling and analysis of a harvested prey-predator system incorporating a prey refuge, *Journal of Computational and Applied Mathematics*, **185**, 19-33 (2006).
- [6] D. Pal, T. K. Kar, A. Yamauchi, and B. Ghosh, Balancing maximum sustainable yield and ecological resilience in an exploited two-predator one-prey system, *BioSystems*, **187**, 1-13 (2020).
- [7] P. Panja, Prey-predator-scavenger model with Monod-Haldane type functional response, *Rendiconti del Circolo Matematico di Palermo Series 2*, DOI 10.1007/s12215-019-00462-9
- [8] T. K. Kar and S. Misra, Optimal control of a fishery under critical depensation, *Journal of Fisheries and Aquatic Science*, **1**, 253-261 (2006).
- [9] B. D. Craven, *Control and Optimization*, CRC Press, New York, 1995.
- [10] C. W. Clark, *Mathematical Bioeconomics: The Mathematics of Conservation*, Wiley, New Jersey, 2010.
- [11] M. B. Schaefer, Some aspects of the dynamics of population importance to the management of commercial marine fisheries, *Bulletin of the Inter-American Tropical Tuna Commission*, **1**, 2, 25-56 (1954).
- [12] M. Ibrahim, An application of optimal control to the marine artisanal fishery in Ghana, *Communications in Mathematical Biology and Neuroscience*, **22**, 1-27 (2019).
- [13] H. S. Gordon, The economic theory of a common property resource, *Journal of Political Economy*, **62**, 124-142 (1954).
- [14] M. Bailey, S. Quatey, A. K. Armah, J. Jacquet, A. Khan, J. Alder, and U. R. Sumaila, *Meeting socioeconomic objectives in Ghana's sardinella fishery*, in *Natural Resources in Ghana: Management, Policy and Economics*, D. M. Nanang and T. K. Nunifu, Ed. Hauppauge: Nova Science Publishers, 293-308 (2011).
- [15] W. H. Fleming and R. W. Rishel, *Deterministic and Stochastic Optimal Control*, Springer Verlag, New York, 1975.
- [16] D. L. Lukes, *Differential Equations: Classical to Controlled*, Academic Press, New York, 1982.
- [17] L. S. Pontryagin, V. G. Boltyanskii, R. V. Gamkrelize and E. F. Mishchenko, *The Mathematical Theory of Optimal Control*, Wiley, New York, 1962.
- [18] P. Cartigny and P. Michel, On a sufficient transversality condition for infinite horizon optimal control problems, *Automata*, **39**, 1007-1010 (2003).
- [19] A. C. Chiang, *Elements of Dynamic Optimization*, McGraw-Hill, Singapore, 1992.
- [20] S. Lenhart and J. T. Workman, *Optimal Control Applied to Biological Models*, Taylor and Francis, Boca Raton, 2007.
- [21] F. M. Hilker, Population collapse to extinction: the catastrophic combination of parasitism and Allee effect, *Journal of Biological Dynamics*, **4**, 86-101 (2010).



mathematics and operations research.

Mahmud Ibrahim earned his PhD degree in Mathematics at the University of Cape Coast, Ghana. He is currently a lecturer in the Department of Mathematics at the University; and his research interests include optimal control, fisheries bioeconomics, computational